SUPPLEMENT TO THE *WELDING JOURNAL*, APRIL 2009
Sponsored by the American Welding Society and the Welding Research Council

Development of a Multiline Laser Vision Sensor for Joint Tracking in Welding

New algorithms improve the reliability and precision in high-speed joint tracking with a multiline laser vision sensor using multiple-range data

BY K. SUNG, H. LEE, Y. S. CHOI, AND S. RHEE

ABSTRACT

In recent years, laser vision sensors have been widely used to track the weld joint. However, they could not be used to detect the joint precisely for high-speed welding. A multiline laser vision sensor (MLVS), which was used in this work overcame the problem.

Five laser lines, which were made by an aspheric lens with a point laser source, provided important information to find the weld joint lines. Clearer images were obtained through the medium, an erosion/dilation filter, and hence, five enhanced range data were obtained by the extraction method.

Through the proposed method, 20 images per second could be processed. Experiments were performed with the MLVS attached to a robot. The weld joint line was tracked with speeds of 10, 15, and 20 m/min, and the mean error was 0.3 mm and a maximum error was 0.6 mm. It was found that this MLVS was very reliable for tracking the weld interface.

Introduction

Laser vision sensors are widely used in automated manufacturing processes in noisy environments, such as welding, because such sensors are robust even in the presence of extreme noise. Smati et al. (Ref. 1), Clocksin et al. (Ref. 2), and Agapakis (Ref. 3) obtained the feature point from the range data of a base metal using a conventional laser vision sensor, and they suggested that the joint can be found and tracked. Since then, Suga and Ishii (Ref. 4) have applied a laser vision sensor in welding process control and automatic welding inspection. Recently, many kinds of high-speed welding processes have been introduced in an effort to improve productivity. If high-energy sources are used in thin-plate welding, it is possible to weld at 10 m/min or faster (Ref. 5).

Laser vision sensors using a high-speed charge-coupled device (CCD) to obtain high-speed performance have been investigated. However, the cost of this is significantly high. The Oxford Sensor Co. (Ref. 6) in England has attempted to achieve reasonable cost along with enhanced reliability by using circular patterns. However, it was then necessary to have separate rotational scanning devices using galvanometers. Also, there are methods that employ multiple laser sources and CCDs (Ref. 7). However, the resulting vision sensor would be large and expensive.

In addition, Lee et al. (Ref. 8) used a high-speed laser vision sensor to detect the weld defects on the shock absorber of a car. A CCD with a speed of 100 ft/s was used to measure the welding part. However, because the laser vision sensor was large and heavy, they chose to fix the laser vision sensor and move the shock absorber. Also, other studies have used multiple laser strips. Kang et al. (Ref. 9) used two lasers to obtain the images of wide area. Park et al. (Ref. 10) also used two lasers with different angles of incidence to solve the problem of the high difference of the angles of the workpieces. Bonser et al. (Ref. 11) studied the method of finding the joint in the saddle of a bicycle using 32 or more laser lines. They inserted the entire welding part into the laser area and imaged the laser lines to find the joint at once. This method can find the joint very quickly, but this is possible only when the welding part is small and cannot be applied if real-time tracking is needed.

In this study, a method was developed to process multiple-range data simultaneously using multilaser patterns in an image. This method produced a high data acquisition rate, even while using a standard CCD. By employing a 5-laser-line pattern using a single laser source and lens, a simple, lightweight sensor structure could be fabricated. The prototype for the multiline laser vision sensor (MLVS) was constructed in this way and applied to tracking the joint for high-speed lap joint welding.

KEYWORDS

Laser Vision Sensor
Image Processing
Joint Tracking
Lap Joint
Multiline Structured Laser
Triangulation

Basic Principles of MLVS

The laser vision sensor obtains range data through optical trigonometry. A MLVS can acquire data for multiple laser lines using the same method employed by single-line laser vision sensors.

Figure 1 shows the basic principles of a laser vision sensor. Figure 1A depicts a conventional laser vision sensor, which projects a line-shaped structural laser onto the workpiece and acquires range data by measuring the form of this laser plane with a CCD. The multiline patterned laser vision sensor shown in Fig. 1B utilizes the same principle to obtain range data, but the latter differs from the former in terms of the image obtained by the CCD. The image from the latter contains multiple laser lines whereas the former contains

K. SUNG is a post-doctor in the School of Mechanical Engineering, Hanyang University, Seoul, Korea, H. LEE and Y. S. CHOI are graduate students and research assistants in the Department of Mechanical Engineering, Hanyang University, Seoul, Korea, and S. RHEE is a professor in the School of Mechanical Engineering, Hanyang University, Seoul, Korea.

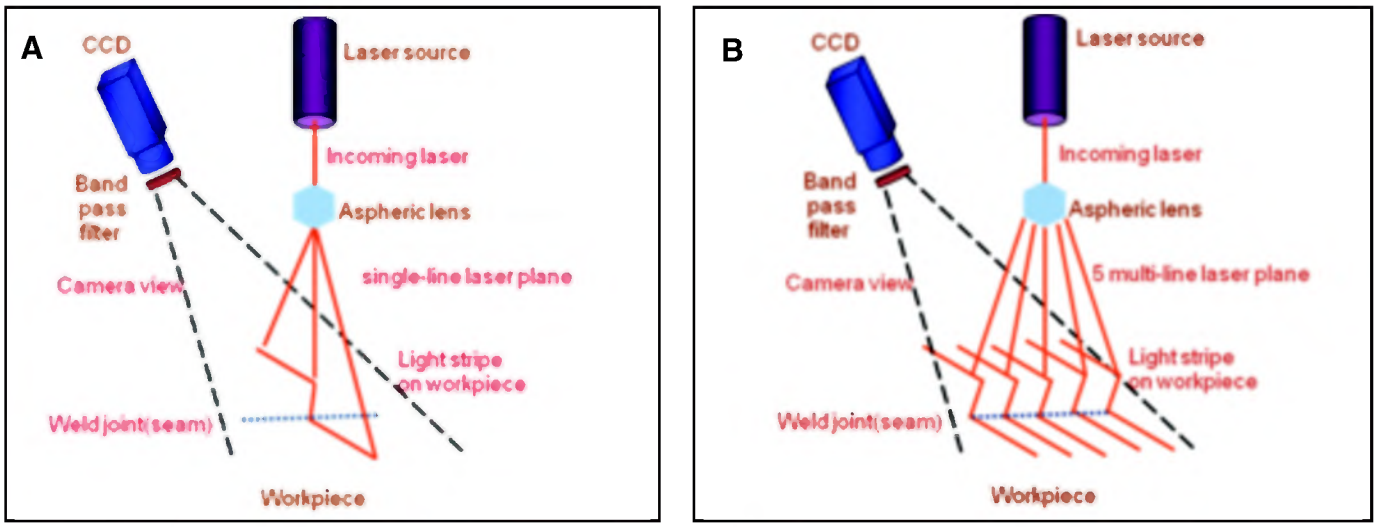

Fig. 1 — Basic configuration of a laser vision sensor. A — Single line; B — multiple lines.

Fig. 2 — Schematic diagram of image processing for multiple laser lines.

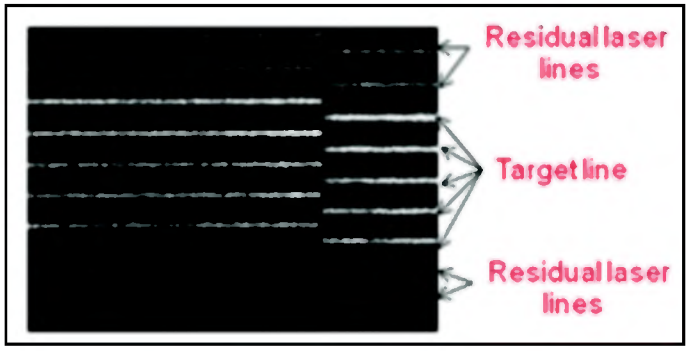

Fig. 3 — Raw image data of the MLVS including noise.

Table 1 — MLVS Validation for High-Speed Lap Joint Tracking

	MLVS : Prototype
Profile fail	1.5%
Valid rate of profile	92.59% (600pixel) 93.21, 93.47, 91.57, 92.05 92.73 (%)
Tracking error	Average: 0.3076 mm Max.: 0.5756 mm

only a single laser line. Therefore, this method requires the additional process of extracting and discriminating multiple laser lines included in the image.

In addition, when the CCD is structurally perpendicular to the ground in the MLVS, each laser plane has a different incidence angle to the workpiece and distance from the starting position to the sensing position, causing the light intensity to change greatly. In such cases, differences in laser line intensity transmitted to the workpiece will increase, and the thickness and intensity of the laser lines generated on each laser plane will vary. Therefore, the MLVS image processing algorithm should take this phenomenon into account. This new image processing algorithm is shown after this section.

Image Preprocessing and Acquisition of Range Data

Laser lines are extracted from the acquired image, and within the laser lines, the range data are determined by processing the line position. To extract laser lines, image preprocessing, laser-line extraction, and feature extraction are generally implemented.

Figure 2 shows the image processing and range data acquisition process of the MLVS. It is similar to that of a conventional laser vision sensor but differs by having the capability to acquire multiple laser lines from an image, corresponding to multiple-range data.

Since the MLVS acquires multiple-range data from an image, the MLVS requires a more complex processing system than conventional systems, for example, sorting the laser lines after image preprocessing. Nevertheless, in our study, image processing was accomplished within an interval of 20 m/s.

Image Preprocessing

The images obtained from the CCD include not only laser lines but also noise due to spatter, arc light, or overlapped reflection. To extract the laser lines precisely, noise in the CCD images must be removed. This process is referred to as image preprocessing. A smoothing filter and a convolution mask are generally used for this in conventional laser vision sensors (Ref. 12).

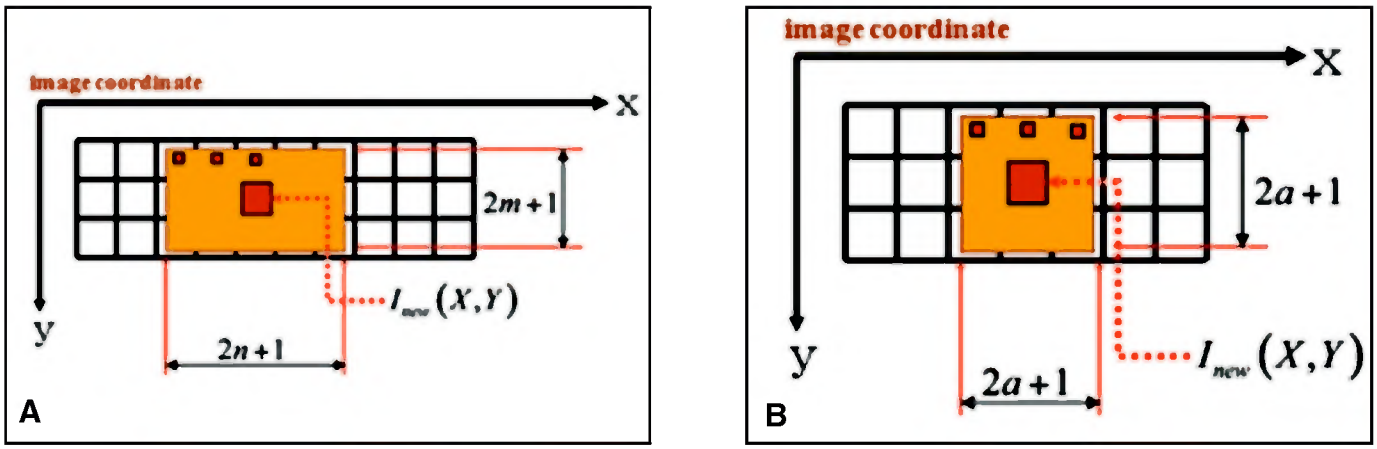

Fig. 4 — Preprocessing filters. A — Advanced median filter mask; B — simplified erosion/dilation filter mask.

In Fig. 3, the additional laser lines, other than the five main lines, are noise. In our system, the point lasers are converted into five main laser lines using an aspheric lens. However, the aspheric lens (Refs. 13, 14) also generates additional noise, which has the same pattern of light intensity as the five main lines, cannot be distinguished from them by a convolution mask. Consequently, a new method is required.

In this study, advanced image preprocessing techniques are proposed. For the first step of preprocessing, an advanced median filter (Ref. 15) was used to remove or reduce the noise within the image. Specialized masks were used for this filter to intensify the laser lines and to weaken the noise. The filter is expressed in Equation 1 and Fig. 4A.

$$I_{new}(X,Y) = \frac{\sum_{j=Y-mi=X-n}^{Y+m}\sum^{X+n} I_{raw}(i,j)}{(2n+1)(2m+1)}$$
$$where\ X = n\cdots(640-n), Y = m\cdots(480-m) \quad (1)$$

In Equation 1, I_{raw} is the raw image intensity from the CCD in the image coordinate, and I_{new} is the image intensity after advanced median filtering. $(2n + 1)$ indicates the pixel number within the mask in the x-axis direction, and $(2m + 1)$ shows the pixel number within the mask in the y-axis direction.

Through this process, spot noise and relatively low-intensity line and area noise were removed. The line noise due to spatter in the orthogonal direction against the laser line was merged into spot noise. To completely remove the remaining noise and to strengthen the laser lines, erosion and dilation filters were also used. Equation 2 is an erosion filter, and Equation 3 is a dilation filter (Ref. 16).

$$I'_{new}(X,Y) = \begin{cases} I_{new}(i,j): if \prod_{j=Y-ai=X-a}^{Y+a}\prod^{X+a} I_{new}(i,j) > 0 \\ 0 \quad : otherwise \end{cases}$$
$$where\ X = a\cdots(640-a), Y = a\cdots(480-a) \quad (2)$$

$$I''_{new}(X,Y) = \begin{cases} \frac{\sum_{j=Y-ai=X-a}^{Y+a}\sum^{X+a} I'_{raw}(i,j)}{(2a+1)^2} : if \sum_{j=Y-ai=X-a}^{Y+a}\sum^{X+a} I'_{new}(i,j) > 0 \\ 0 \quad : otherwise \end{cases}$$
$$where\ X = a\cdots(640-a), Y = a\cdots(480-a) \quad (3)$$

In Equation 3, I''_{new} is the image intensity after the erosion and dilation filtering. In Fig. 4B, each mask size of the erosion and dilation filter is the same at $(2a + 1)$.

Finally, an advanced half-thresholding method was used to reinforce the contrasts of the intensity (Ref. 17). This made the extraction of laser lines from the image easy. Figure 5 shows the advanced half-thresholding method that was implemented using Equation 4 for each of the Y values. In Equation 4, I represents the final image after advanced half-thresholding. In Equation 5, n is the pixel number of the mask in the direction of the y-axis.

$$I(X,Y) = \begin{cases} 0 \ \ if\ I''_{new}(i,Y) < th-value, (i = 0\cdots640) \\ I''_{new}(i,Y) \quad otherwise \end{cases} \quad (4)$$

where,

$$th-value = \max\left[\frac{\sum_{k=j-n/2}^{j+n/2-1} I''_{new}(k,Y)}{n} \times 0.7\right],$$
$$\left(j = n/2\cdots(640-n/2)\right) \quad (5)$$

Line Discrimination and Extraction Process

Laser line data were extracted from the image after image preprocessing. Then, each single laser line was discriminated from the other extracted laser lines and was converted into range data. The laser lines were properly ordered to enable extraction of accurate range data.

Following preprocessing, the image was divided into black parts and nonblack parts. It was assumed that any areas other than the black parts within the image were composed of laser lines.

The time available for image processing was limited; therefore, a new algorithm was developed that could extract and discriminate the laser lines simultaneously. Figure 6 shows that the preprocessed image was converted into 5 discriminated laser lines by the extraction and discrimination method.

The column intensity was used for extracting laser lines. As in Fig. 7A, the A-A' line had a width of 1 pixel. The A-A' line is expressed as a column intensity, as in Fig. 7B. The column intensity is represented at $I_k(i)$, where k is the column number along the x-axis in the image coordinates (Fig. 7A) and i is the position of the x-axis in the column intensity function — Fig. 7B.

There are additional laser lines beyond the main five lines, as shown in Fig. 3. To eliminate such noise, it is necessary to determine the peak points and to select the valid groups as shown in Fig. 8. This process consists of the following tasks: determining the peaks from the column intensity, grouping the peaks sequentially by decreasing the intensity, and selecting the group of peaks that has the highest mean intensity. If such a process is applied to each pixel column, a collection of laser lines is obtained for each column.

Extraction of Feature Point

Range data represent the cross-sectional form of a workpiece. A simple

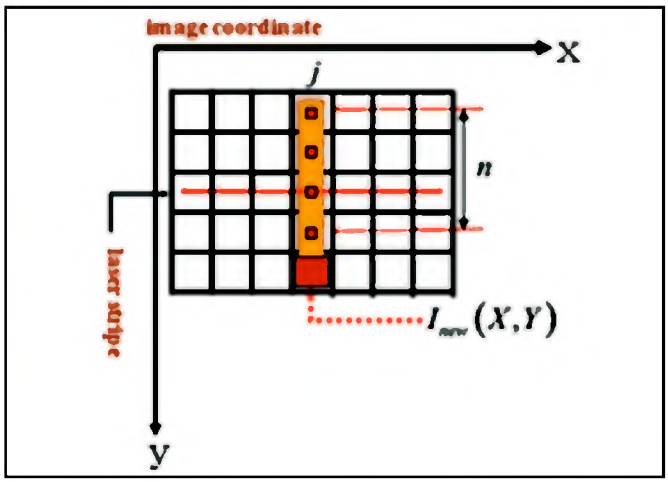

Fig. 5 — Advanced half-thresholding method.

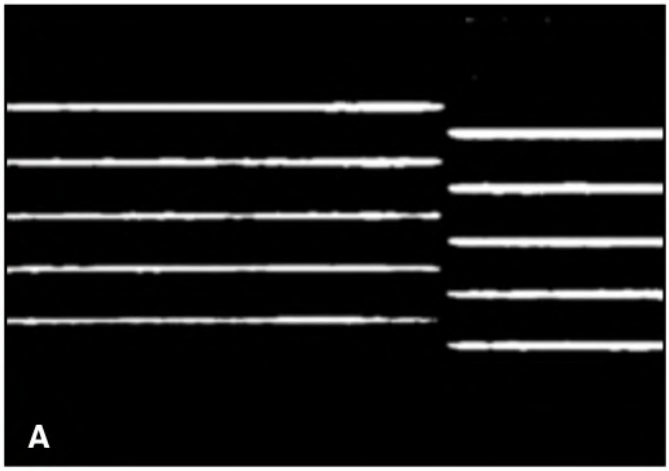

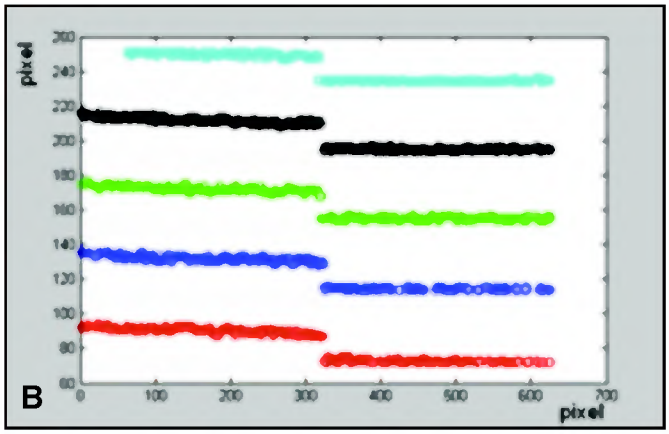

Fig. 6 — Line extraction and discrimination from a preprocessed image. A — Processed image data; B — discriminated laser profile data.

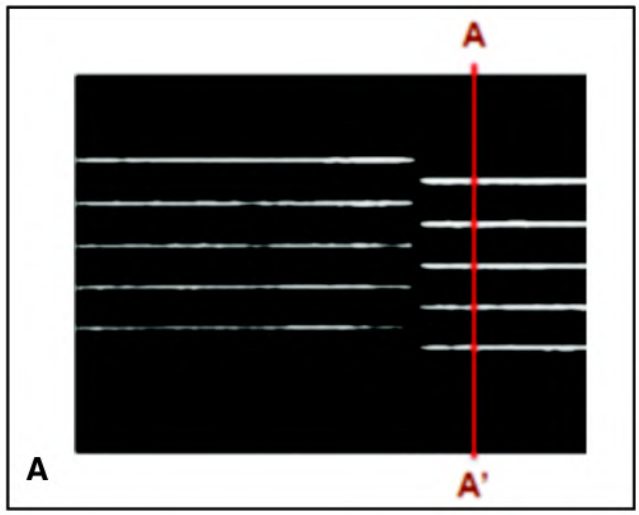

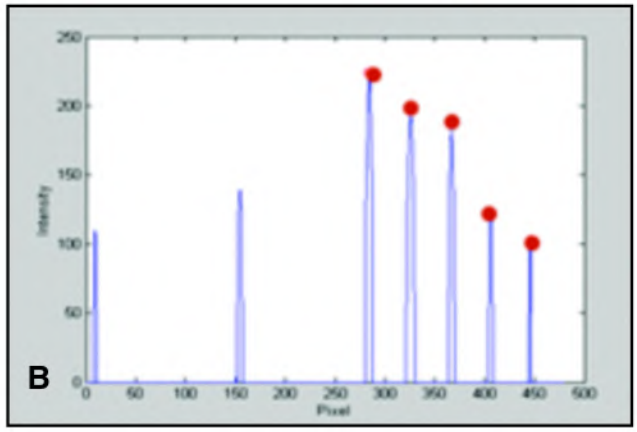

Fig. 7 — Determination of the column intensity from processed image data. A — Processed image data; B — column intensity for section A-A'.

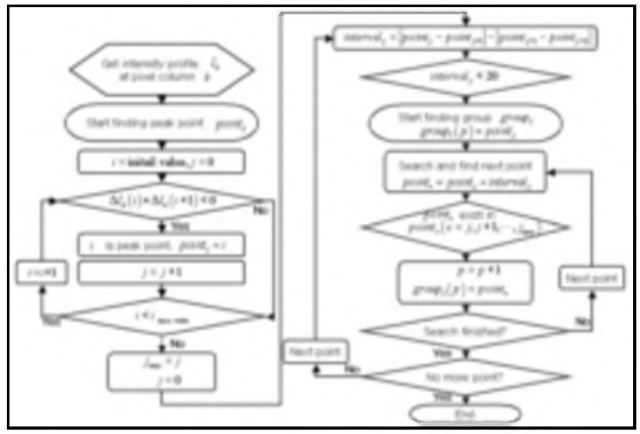

Fig. 8 — Flow chart for the line discrimination and extraction process.

template matching method is used to track the joint (specific point) (Ref. 18). This method extracts the feature points from the range data. Because the MLVS was applied to lap joint joint tracking, two horizontal lines and one sloped line were used, as shown in Fig. 9.

The traditional "split and merge" method was adapted for feature extraction in this study (Ref. 19). The adopted split and merge method employs a technique that generates straight lines based on three points and then measures the angles among them. This method can minimize errors near the feature points and increase the processing speed.

Because we used the split and merge method, the merged point in Fig. 10 is unified in a straight line if the angles of the line stay near 180 deg, as shown in Fig. 11A. As indicated in Fig. 11B, a noise that is a white point in Fig. 10 is removed when the angle between the two lines exceeds a certain threshold. If the method is repeated, only the feature points, which are solid, will remain in the end. Thus, the template is matched with the feature points, and the tracking point is found.

The joint was constructed by determining the trends of the tracking points. The

MLVS relies on measured fields that partially overlap; hence, tracking errors could be detected through a comparison of current tracking points with prior tracking points, enabling the MLVS to safely track the joint even at higher speeds.

MLVS System

The MLVS system consists of a laser source, aspheric lens, and CCD camera. The laser used for MLVS was a IIIb-class diode laser with power of 100 mW and wavelength of 650 nm. An aspheric lens made by StockerYale, Inc., was used to generate five laser strips. This aspheric lens can generate five laser lines at 120 mm, which are 7 mm apart. A ½-in. CCIR CCD with 640 × 480 pixels was also used to capture the maximum 30 frames per second. A 650-nm band pass filter with band width of 10 nm was installed in this device. This sensor is shown in Fig. 12.

To process the incoming images in the CCD, image grabber Meteor MC was used (Ref. 20). The digital images were obtained from analog images with this grabber. An industrial computer was used to process images and calculate robot motions. The image processing program was written on the basis of C++. Also, for real-time tracking, the image processing program was created in such a way as to be integrated into the robot control program.

The horizontal and vertical resolutions of MLVS were 0.06 mm. The MLVS software includes an image processing program that is capable of processing more than 20 frames per second. In terms of a conventional single-line laser vision sensor, this would be the equivalent of more than 100 frames per second.

Results

Experimental Setup

The weld joint tracking system was composed of a Samsung 6-axis welding robot, the fabricated MLVS, and an industrial PC with image grabbing board as shown in Fig. 13. If the joint was very long, the 4-axis bogie-type robot was used. The industrial PC received image signals from the MLVS and performed image processing and analysis; in addition, the PC played a role in controlling the robot through the Ethernet, and in using the subsequent results. The software for these functions was developed as part of our study.

Results of Joint Tracking

Figure 14 shows the laser lines projected onto the workpieces by the MLVS, and the images acquired from the workpieces are depicted in Fig. 15A. The images before preprocessing noticeably include a great deal of noise in addition to the laser lines. Figure 15B demonstrates the features of noise removal and the reinforcement of the laser lines by the advanced median filter. In a subsequent stage, the erosion/dilation filter was able to reduce the remaining noise even further while subtly enhancing the laser lines. Finally, images could be acquired without noise, as shown in Fig. 15C, using the half-threshold method developed for this study.

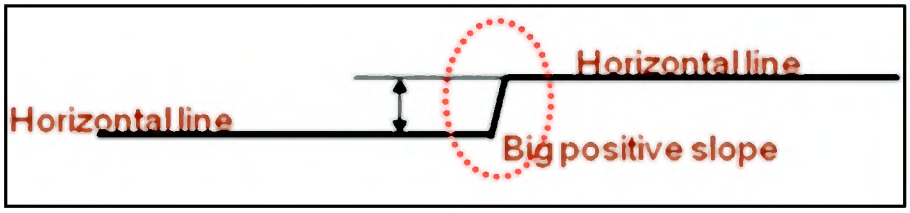

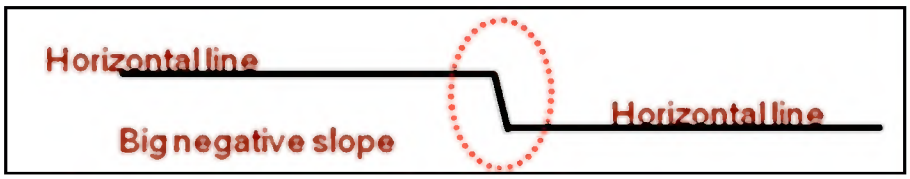

Fig. 9 — Lap joint template for feature extraction. A — Big positive slope; B — big negative slope.

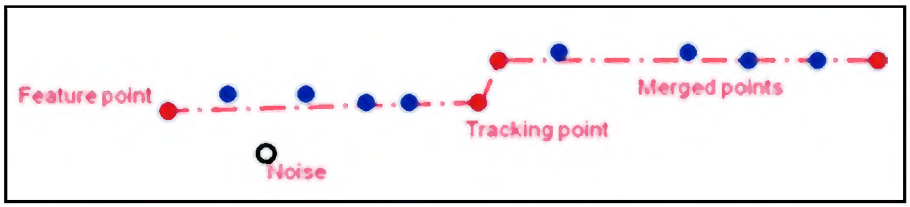

Fig. 10 — Advanced "split and merge" algorithm for the plane surface in a welded joint.

An experiment to obtain range data in a straight-line lap joint was conducted. The experiment checked the image processing algorithm of the MLVS and the accuracy of the range data extraction. Range data were obtained while moving along a 1-meter path 5 times at each of the following speeds: 10, 15, and 20 m/min. Figure 16 shows the range data obtained from MLVS at 15 m/min tracking speed. The x marks in Fig. 16 are tracking points.

The probability of obtaining false range data was 7.4% on average, according to the experiment. Thus, about 44 points were incorrectly positioned among 600 points in one set of range data. However, most of the incorrect points were positioned near the beginning or end of the range (#1~50 or #550~600 pixel data positions). The beginning and end of the range data are relatively less important than the other parts.

It would be possible to examine the mutual relationships among the five laser lines, and to modify them, so as to remove additional errors. After completing this, the probability of errors in the range data created by the laser line would be less than 1%.

The "Profile fail" in Table 1 indicates a case where one of the frames obtained only incorrectly positioned welding parts in the aforementioned experiment. These were mainly cases involving errors in the range data for the fifth laser line. There were no cases in which a preponderance of range data involving all five laser lines caused incorrectly positioned welding parts. The "valid rate of profile" is the rate of the number of range data points normally obtained in the range data acquired from a frame. It is assumed that the weld joint is a completely straight line and that there are no robot tracking errors. When generating the robot's welding path by extracting tracking points from range data under this assumption, the "tracking error" is the difference of the robot's welding path from the weld joint.

The results demonstrated that the MLVS could extract five range data values simultaneously from a frame by using the new image processing method and range data extraction algorithm while employing existing hardware. Such range data were found to be accurate and was obtained quickly enough to support tracking applications using robots.

The laser vision sensor is located in front of the welding gun to extract the joint in advance. For a single-line LVS, the

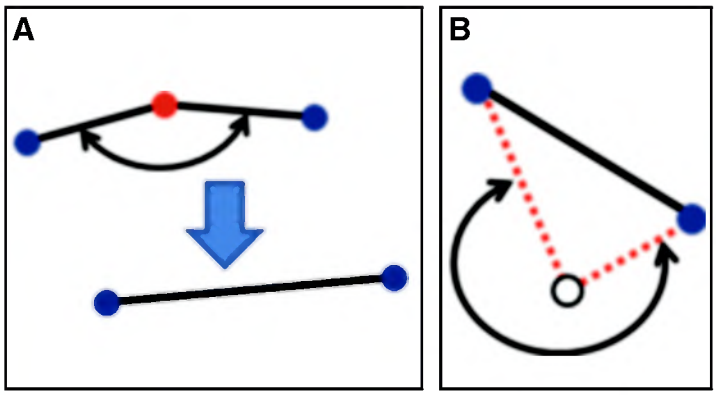

Fig. 11 — Advanced split and merge feature extraction algorithm for joint tracking. A — Simplified split and merge polygonal approximation; B — noise detection using polygonal approximation.

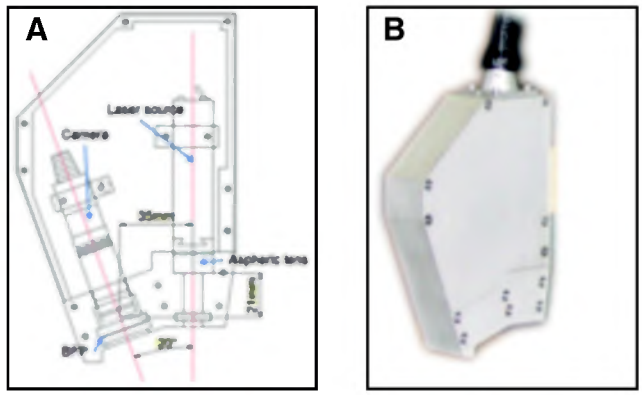

Fig. 12 — Design and fabrication of MVLS. A — Design of MVLS; B — fabricated prototype MVLS.

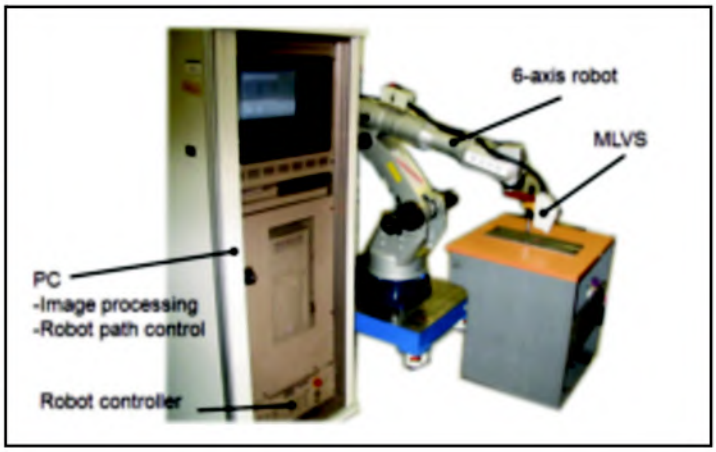

Fig. 13 — Joint tracking system configuration.

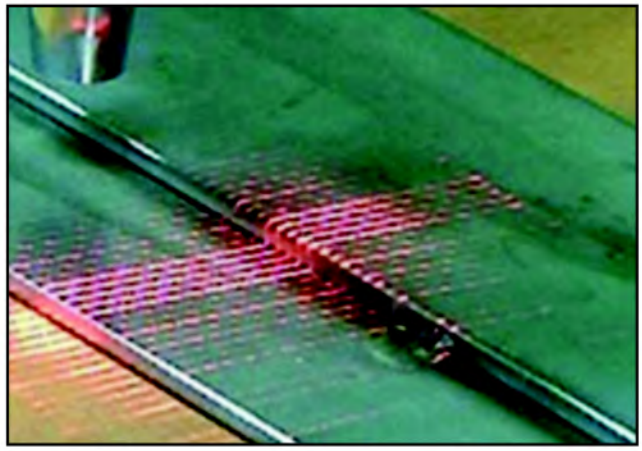

Fig. 14 — Projected laser stripes.

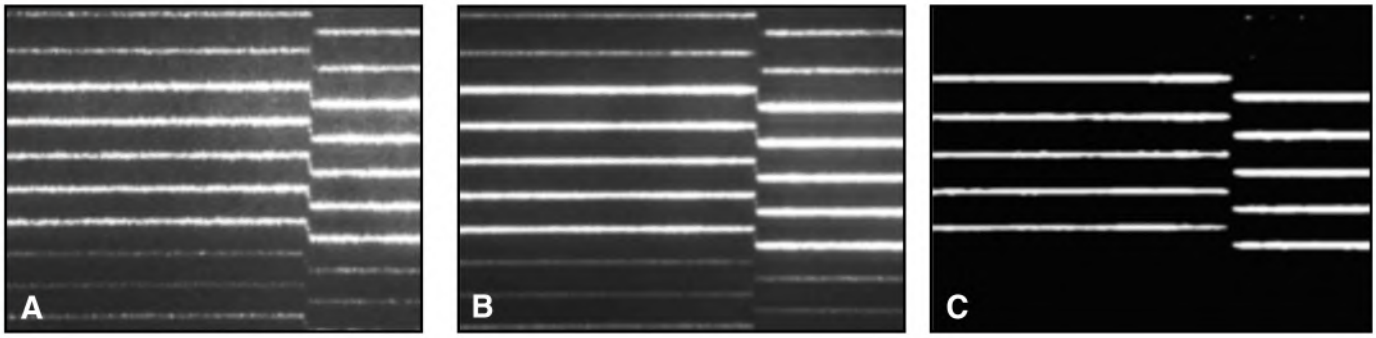

Fig. 15 — Image processing procedure. A — Raw data; B — used advanced median filter; C — final image

data for the joint line were obtained at intervals of 5 mm for a welding speed of 10 m/min. In the case of MLVS, the information for the joint line was obtained every 2 mm. Therefore, a more accurate and stable joint tracking was possible.

Conclusions

In this study, we developed a multiline laser vision sensor that improved the tracking capability and reliability of conventional laser vision sensors so as to apply high-speed joint tracking. New algorithms applied in the MLVS enabled multiple range data to be obtained concurrently within a single image by using multiple laser stripes.

To increase the reliability and precision in high-speed joint tracking, the MLVS uses multiple-range data. In this study, a single laser optical system and a single CCD were used to obtain multiple-range data from an image. This process can be modified to be compact so that it would be suitable for an automatic system.

Since the MLVS acquires multiple-range data from an image, the adapted preprocessing method was advanced to be suitable for this research. Also, a new algorithm was developed to extract and discriminate the laser lines from the preprocessed image. Advanced prepro-

cessing adapted a median filter and an erosion/dilation filter that were modified to be suitable for this study. A new method to threshold, half-thresholding, was proposed to make an easier line separation and extraction process.

To minimize the processing time, a new algorithm was developed to extract and discriminate the laser lines simultaneously. This algorithm enables ranges to be distinguished, which are considered to be the laser lines within the image, and put the most suitable laser lines into the valid group by comparing each line with the patterns. The whole image processing was accomplished within 20 ms, and the range data have 93% accuracy on average.

In this study, a prototype MLVS was designed and fabricated using a conventional CCD. A simple template matching method was used to determine tracking points using the feature extraction algorithm. Determined tracking points were transmitted to the welding robot by using the Ethernet. This system was constructed and applied in high-speed (max. 20 m/min) joint tracking in a lap joint and tracked a joint successfully, less than 0.3 mm average error.

This study conducted the MLVS at nearly the same size and cost of the previous laser vision sensor and increased the precision and reliability of high-speed joint tracking by acquiring multiple-range data within an image.

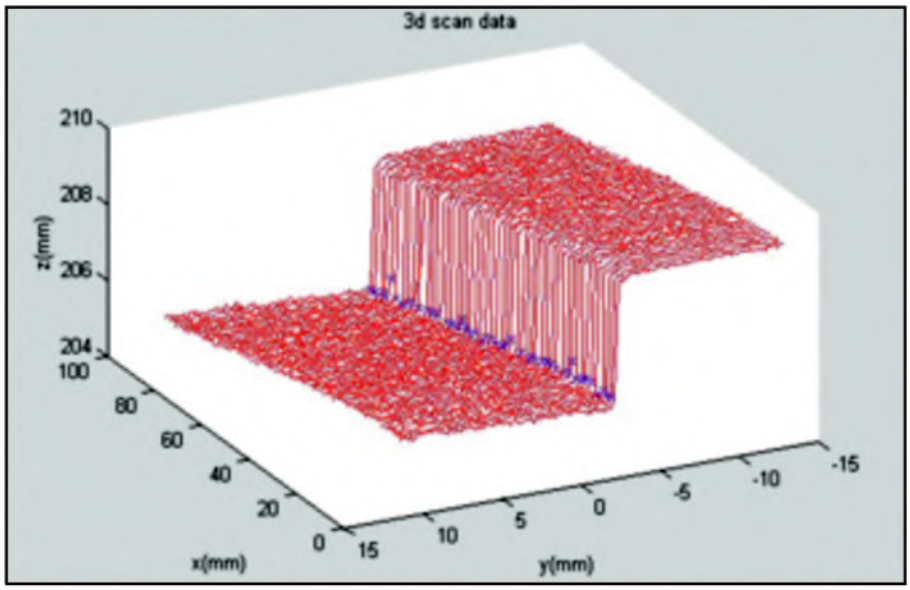

Fig. 16 — Three-dimensional information of the weld joint and workpiece.

Acknowledgments

This work was supported by the strategic industrial innovation cluster supporting project of Seoul City, Korea. It was also supported by the Second Brain Korea 21 Project in 2008.

References

1. Smati, Z., Yapp, D., and Smith, C. J. 1983. An industrial robot using sensory feedback for an automatic multi-pass welding system. *Proceeding British Robot Association* 6: 91–100.

2. Clocksin, W. F., Bromley, J. S. E., Davey, P. G., Vidler, A. R., and Morgan, C. G. 1985. An implementation of model based visual feedback for robot arc welding of thin sheet steel. *The International Journal of Robotics Research* 4: 13–26.

3. Agapakis, J. E., Katz , J. M., Friedman, J. M., and Epstein, G. N. 1990. Vision-aided robotic welding: An approach and flexible implementation. *The International Journal of Robotics Research* 9(5): 17–34.

4. Suga, Y., and Ishii, A. 1998. Application of image processing to automatic weld inspection and welding process control. *The Japan Society of Precision Engineering* 32(2).

5. Park , S. J., Jang, U. S., Chun, C. K., and Ju, S. M. 2006. High speed key-hole welding by fiber laser. *Journal of the Korean Welding Society* 46: 195–197.

6. *www.oxfordsensor.com*, Oxford Sensor Co., Ltd.

7. Kim, P., Rhee, S., and Lee, C. H. 1999. Automatic teaching of welding robot for free-formed seam using laser vision sensor. *Optics and Lasers in Engineering* 31(3): 173–182.

8. Lee, H., Sung, K., Park, H. and Rhee, S. 2004. Measurement of weld bead defect for shock absorber using laser vision sensor. *Key Engineering Materials* 270-273: 2332–2337.

9. Kang, M.-G., Kim, J.-H., Park, Y.-J. and Woo, G.-J. 2007. Laser vision system for automatic seam tracking of stainless steel pipe welding machine. *International Conference on Control, Automation and Systems*. pp. 1046–1051,

10. Park, K., Kim, Y., Byeon, J., Sung, K., Yeom, C. and Rhee, S. 2007. Development of an auto-welding system for CRD nozzle repair welds using a 3D laser vision sensor. *Journal of Mechanical Science and Technology* 21(10): 1720–1725.

11. Bonser, G., and Parker, G. A. 1999. Robotic gas metal arc welding of small diameter saddle type joints using multistripe structured light. *Optical Engineering* 38(11): 1943–1948.

12. Agapakis, J. E. 1990. Approaches for recognition and interpretation of workpiece surface features using structured lighting. *The International Journal of Robotics Research* 9(5): 3–16.

13. *www.stockeryale.com/i/ lasers/ products /snf.htm,* Lasiris™ SNF Lasers.

14. Richard A. F. 1992. Line Projector Lens. U.S. Patent 5283694.

15. Haralick, R. M., and Shapiro, L. G. 1992. *Computer and Robot Vision*, Vol. I. Addison-Wesley Publishing Co., Inc.

16. Gomes, J., and Velho, L. 1997. *Image Processing for Computer Graphics*. Springer-Verlag, New York.

17. Eiho, S., and Qian, Y. 1997. Detection of coronary artery tree using morphological operator. *Computers in Cardiology*, pp. 525–528.

18. Kim, P., Rhee, S., and Lee, C. H. 1999. Automatic teaching of welding robot for free-formed seam using laser vision sensor. *Optics and Lasers in Engineering* 31(3): 173–182.

19. Xiao, Y., Jia Zou, J. and Yan, H. 2001. An adaptive split-and-merge method for binary image contour data compression. *Pattern Recognition Letters* 22(3-4): 299–307.

20. *www.matrox.com*, Meteor MC.

Correction

In the research paper authored by R. Rai et al., which appeared on pages 54-s to 61-s of the March issue, two of the references are incorrect. The Welding Journal regrets the error. The correct references follow:

41. Kim, C. H., Zhang, W., and DebRoy, T. 2003. Modeling of Temperature Field and Solidified Surface Profile during Gas Metal Arc Fillet Welding. Journal of Applied Physics 94(4): 2667 to 2679.

42. De, A., and DebRoy, T. 2004. Probing Unknown Welding Parameters from Convective Heat Transfer Calculation and Multivariable Optimization. Journal of Physics D: Applied Physics 37(1): 140 to 150.